PB86-218112

# Modeling of the Upper and Lower Respiratory Systems

Northrop Services, Inc.
Research Triangle Park, NC

Prepared for

Health Effects Research Lab.
Research Triangle Park, NC

Jun 86

U.S. Department of Commerce
National Technical Information Service
NTIS

PB86-218112

EPA/600/D-86/126
June 1986

# Modeling of the Upper and Lower Respiratory Systems

by

Amit L. Patra
Northrop Services, Inc.--Environmental Sciences
Research Triangle Park, NC 27709

EPA Contract
68-02-4032

EPA Project Officer
Fred J. Miller

HEALTH EFFECTS RESEARCH LABORATORY
OFFICE OF RESEARCH AND DEVELOPMENT
U.S. ENVIRONMENTAL PROTECTION AGENCY
RESEARCH TRIANGLE PARK, NC 27711

REPRODUCED BY
NATIONAL TECHNICAL
INFORMATION SERVICE
U.S. DEPARTMENT OF COMMERCE
SPRINGFIELD, VA. 22161

**TECHNICAL REPORT DATA**
*(Please read Instructions on the reverse before completing)*

| | |
|---|---|
| 1. REPORT NO. EPA/600/D-86/126 | 2. |
| 3. RECIPIENT'S ACCESSION NO. | |
| 4. TITLE AND SUBTITLE MODELLING OF THE UPPER AND LOWER RESPIRATORY SYSTEMS | 5. REPORT DATE June 1986 |
| | 6. PERFORMING ORGANIZATION CODE |
| 7. AUTHOR(S) A.L. Patra | 8. PERFORMING ORGANIZATION REPORT NO. |
| 9. PERFORMING ORGANIZATION NAME AND ADDRESS Northrop Services, Inc. Research Triangle Park, NC 27709 | 10. PROGRAM ELEMENT NO. |
| | 11. CONTRACT/GRANT NO. 68-02-4032 |
| 12. SPONSORING AGENCY NAME AND ADDRESS Office of Research & Development Health Effects Research Laboratory - RTP, NC U.S. Environmental Protection Agency Research Triangle Park, NC 27711 | 13. TYPE OF REPORT AND PERIOD COVERED |
| | 14. SPONSORING AGENCY CODE EPA-600/11 |

15. SUPPLEMENTARY NOTES

16. ABSTRACT

Casting of silicone rubber replica casts of upper respiratory airways including nose, larynx, trachea, and tracheobronchial airways is described for the human and for standard laboratory animals. Morphometric measurements were made on nasopharyngeal and tracheobronchial airway casts. Cross-sectional areas of nasopharyngeal airways were observed to be complex in nature; each species exhibited different branching patterns and numbers of lobes. Replica casts were used to understand anatomical differences in nose and lung due to parameters such as age, sex, airway branching patterns, and morphometric dimensions. Effects of growth on morphometric dimensions were shown to be highly significant for use in extrapolating toxicological results from one age group to another. Species and strain differences in morphometric dimensions were also observed. Use of replica casts for velocity distribution pattern studies and for particle deposition efficiencies studies were investigated.

17. KEY WORDS AND DOCUMENT ANALYSIS

| a. DESCRIPTORS | b. IDENTIFIERS/OPEN ENDED TERMS | c. COSATI Field/Group |
|---|---|---|
| | | |

| | | |
|---|---|---|
| 18. DISTRIBUTION STATEMENT RELEASE TO PUBLIC | 19. SECURITY CLASS *(This Report)* UNCLASSIFIED | 21. NO. OF PAGES 31 |
| | 20. SECURITY CLASS *(This page)* UNCLASSIFIED | 22. PRICE |

EPA Form 2220-1 (Rev. 4-77) PREVIOUS EDITION IS OBSOLETE

NOTICE

This document has been reviewed in accordance with U.S. Environmental Protection Agency policy and approved for publication. Mention of trade names or commercial products does not constitute endorsement or recommendation for use.

**ABSTRACT**

Casting of silicone rubber replica casts of upper respiratory airways including nose, larynx, trachea, and tracheobronchial airways is described for the human and for standard laboratory animals. Morphometric measurements were made on nasopharyngeal and tracheobronchial airway casts. Cross-sectional areas of nasopharyngeal airways were observed to be complex in nature; each species exhibited different branching patterns and numbers of lobes. Replica casts were used to understand anatomical differences in nose and lung due to parameters such as age, sex, airway branching patterns, and morphometric dimensions. Effects of growth on morphometric dimensions were shown to be highly significant for use in extrapolating toxicological results from one age group to another. Species and strain differences in morphometric dimensions were also observed. Use of replica casts for velocity distribution pattern studies and for particle deposition efficiencies studies were investigated.

## INTRODUCTION

Laboratory animals are commonly used in inhalation toxicology studies as surrogates for humans. The extent and location of deposited inhaled particles in the respiratory tract is a major factor in a particle's toxicity, making the knowledge of anatomical morphometry of species used an integral part of the study. The nasopharyngeal, tracheobronchial, and pulmonary regions make up the mammalian respiratory system. When particles are inhaled, their fractional deposition in different regions of the respiratory tract depends on their aerodynamic properties and on breathing and anatomical characteristics. Gross dissection (2), transverse serial sections (19), and computed tomography (10), among other techniques, have been used by various investigators in the study of respiratory tract anatomy. Replica casts have been used to describe accurately the anatomical details of the respiratory airways. Although upper respiratory tract morphometric data are limited (24,12,11), lower respiratory and solid replica casts have been used by Weibel (26), Horsfield and Cumming (7), and Raabe et al. (17), among others, to study conducting airway geometries. Phalen et al. (16) developed a method to cast lungs *in situ*. Kliment (8) used latex to produce flexible solid lung casts for morphometric measurements. Preparation of a hollow cast was described by Timbrell et al. (25) and modified for particulate deposition studies by Schlesinger and Lippmann (21). Differences in diameters, lengths, branching angles, etc., of the conducting airways have been shown for various strains of the same species (6,17). Schreider (22), Patra (11), and Patra et al. (12) presented detailed comparative anatomy and functions of the nasal passages for different species primarily through the use of replica casts.

Epidemiological evidence shows that children face more environmental risks than adults, but limited quantitative information on deposition data is currently available because controlled exposure studies for these groups are not feasible. There are inherent limitations with *in vivo* human research, thus making it difficult to determine pollutant dosimetric relationship. Limited information on bronchial or nasopharyngeal dimensions in children has been published. Phalen et al. (15) reported morphometric measurements of 20 replica casts from humans aged 11 days to

21 years. They concluded that under normal circumstances younger people will have greater tracheobronchial deposition efficiencies than older people. Unfortunately, a data base for this special group is limited to the tracheobronchial region. Nasopharyngeal data for young humans have only been reported by Patra et al. (12).

An anatomical model of the total repiratory tract is necessary to describe the fluid flow, particle deposition, pressure drop characteristics, etc. Our present work identifies techniques for obtaining solid and hollow replica casts of nasopharyngeal and tracheobronchial airways, the insides of which are identical to the inside of the actual nose and lung specimen. Possible relationships between common mammalian species are discussed. Patterns of airway growth in a single species as a function of age are investigated, and also the influence of nasal and lung airway growth on particle deposition is observed. Also, a hollow nose cast made from a baboon nose is used to study the velocity profiles in the different locations of the nose. The average velocities and velocity profiles were obtained placing thermistor probes in the nasal cavity model, and the data obtained were compared with published data. Data from studies of particle deposition in a hollow child lung replica cast have been compared with computer simulation and published adult lung particle deposition data.

## METHODS

*Cast Preparation*: Replica casts of airways have been validated by different investigators over time (17,11,16,21); they were used in this study for morphometric measurements. The quality of prepared casts depends on the casting material, autopsy specimen, and casting techniques. Resin casts were used by Engle (3) and Horsfield and Cumming (7), epoxy and Cerrolow-117 alloy casts were prepared by Schreider and Hutchens (23), and silicone rubber castings were produced by a number of investigators (17,11,16, 21). In this study, Dow Corning 734 RTV silicone rubber (Dow Corning, Midland, MI) was used for casting airways because of its replicative ability, minimal (< 1%, [16]) shrinkage, flexibility, self-leveling, and room-temperature curing chemistry. The specimens

used in this study were from autopsy human specimens with no known respiratory abnormalities, from healthy primates (Duke Primate Center, Durham, NC), and from laboratory-bred animals (rat, hamster, etc; Charles River Breeding Laboratory, Wilmington, MA). The Rahn and Ross (19) formalin fix method and the Phalen et al. (16) *in situ* casting techniques were modified for this study. For smaller laboratory animals, the *in situ* techniques were found to be more suitable, while excising-fixing-casting techniques were more appropriate for larger primates or human species. The species investigated are listed in Table 1. For casting the airways, a dispensing cylinder was used to inject the pre-measured silicone rubber at a pressure of 0.35 MPa, according to the method described by Patra et al. (14). For *in situ* casting, silicone rubber was injected through a tracheal cannula, and for fixed lungs, silicone rubber was injected through the trachea. Once cured, the casts were digested in sodium hydroxide. They were then rinsed, dried, and pruned for measurement of terminal bronchioles. Figure 1 shows silicone rubber casts of (a) human nose and (b) human lungs. Silicone rubber hollow replica casts of a child's lung and of a baboon nose were developed for particle deposition study according to the methods described elsewhere (14).

*Morphometric Measurements on Casts:* In the tracheobronchial region, each airway measured was identified by a binary numbering system of Phalen et al. (16). A Spencer dissecting scope (American Optical Company, Buffalo, NY) with low magnification (10X) lens (Leitz, Wetzler) was used to measure the length and diameters of the individual airways. The branching angles were measured using a comparator with $\frac{1}{4}^{\circ}$ marking. Three different morphometrists independently measured the airways. In a blind test, numerical values were within 2% for 95% of the time suggesting good comparability among them. Generation numbers have been used according to Weibel convention (26); the trachea as generation 0, the main bronchi as generation 1, and so on down the tracheobronchial tree. The first six generations of airways have been measured in their entirety.

In the nasopharyngeal region, following gross examination, cross sections of the casts were made at various points along their lengths at approximately 3-mm intervals. Separate cross sections

**TABLE 1. Characteristics of species from which replica casts were made**

| Species | Sex | Body Weight | Remarks |
|---|---|---|---|
| Rat | M | 253 g | C-D (12) |
| Rat | M | 365.8 g | F-344 |
| Human | M | 99.8 kg | Nose Study (Figure 1) |
| Baboon | M | 30 kg | $O_3$ exposed (12) |
| Human | M | 33.14 kg | Particle Deposition Study (Figure 6) |
| Human | M | 80 kg | NYU data (21) |

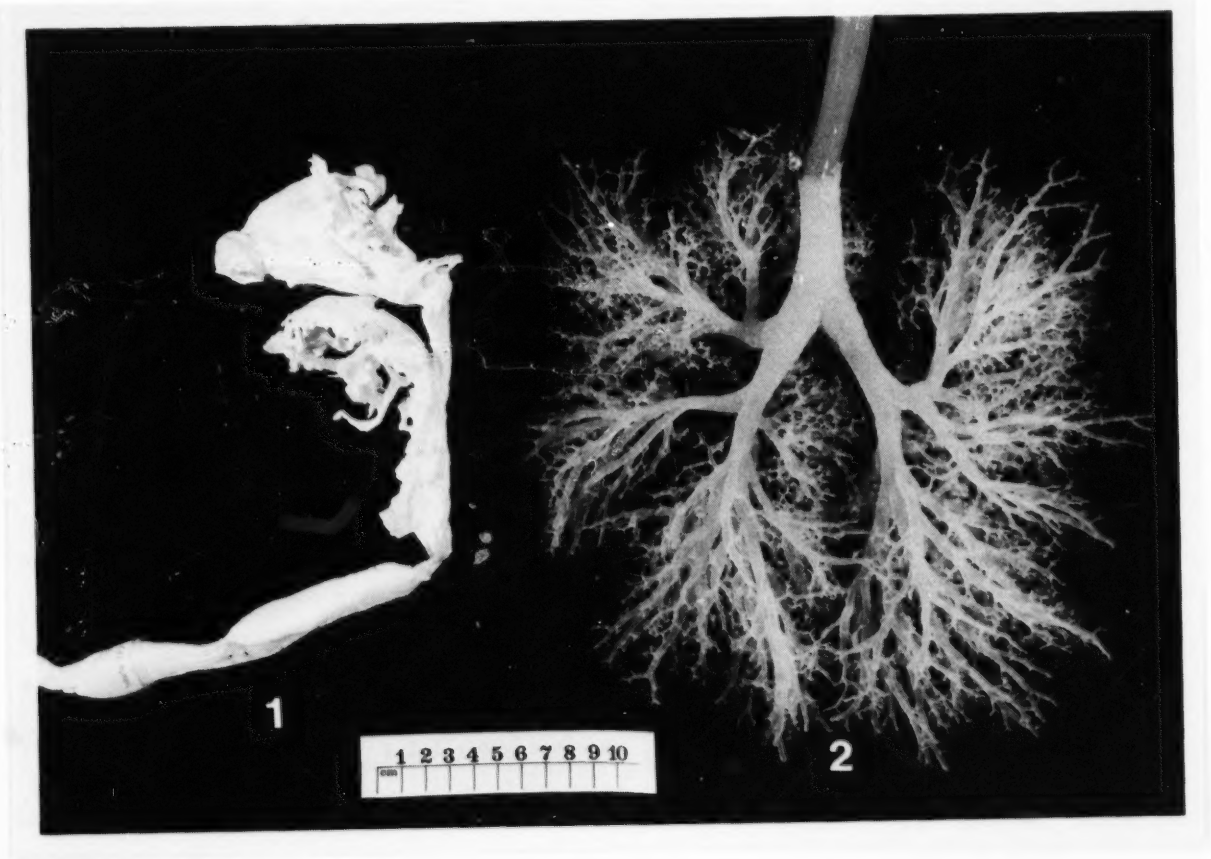


Figure 1. Silicone rubber replica casts of (A) nasopharyngeal region and (B) tracheobronchial region made *in situ* in an adult male (99.8 kg), 39 years old.

were made of both sides of the nose until the two sides joined to form a single unit; cross sections were then made of the entire casts. Full-size (X2.37) replicate drawings of the cross sections were made. Figure 2 shows lateral views of the silicone rubber casts of the sections for an adult Long-Evans hooded rat. Using a Micro-Plan II image analysis system (Laboratory Computer Systems, Inc., Cambridge, MA), the cross-sectional areas and perimeters were measured for each section. The surface area was calculated with the assumption that the thickness of each section was small enough to be considered uniform. Table 2 tabulates these values for the rat nasopharyngeal sections of Figure 1.

*Data Reduction:* This study partially responded to the variability in airway dimensions. After realizing the unavailability of required specimens, we decided to perform age-specific dependence on airway formation in rats and then to make a comparison with available human data from literature. Age and body weight were measured as independent variables, and perimeter and cross-sectional areas in nose, airway length, diameter, and branching angle in the lung were measured as dependent variables. Plots of the data for Fischer-344 and Long-Evans hooded rats to describe the relationship between tracheal dimensions and age are shown in Figure 3. Figure 4 shows perimeter vs. normalized nose length for Fischer-344 and Sprague-Dawley rats. A clear line of anatomical separation was not possible in the case of a nose cast, thus an approximate division of regions was noted following the Schreider et al. (24) convention.

To obtain a velocity profile at a particular location and direction in the extrathoracic region, a thermistor probe (GB 31J1, Fenwal Electronics, Farmingham, MA) placed in a small brass tube (ID 0.4 cm) that acted as a guide for traversing, was inserted inside the model. The hole was then sealed off with silicone rubber putty. The whole setup was adjusted inside the wind tunnel so that flow at the entrance of the nose was 1500 ml/s, and the velocity was recorded as a function of voltage. Each point was repeated three times and averaged. Mapping of the velocity profile was achieved by probe increments of 1-mm steps with a micrometer. The velocity ($v_o$) just outside the tip

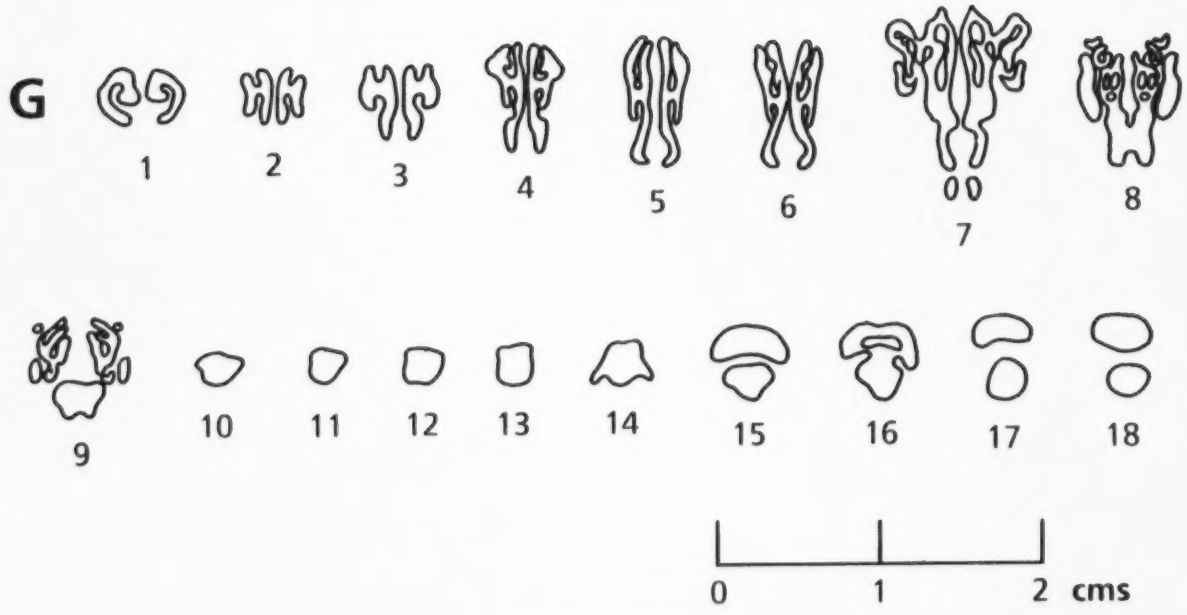


Figure 2. Cross sections of a nasal-pharyngeal airway cast of a Fischer-344 rat. The section numbers correspond to the value in Table 2.

TABLE 2. Morphometric measurements of the cross sections of the nasopharyngeal cast of a Long-Evans Hooded Rat. The section number corresponds to section number in Figure 2.

| Section No. | Distance from the nose tip (mm) | Perimeter (mm) | Area $(mm)^2$ |
|---|---|---|---|
| 1 | 1.70 | 29.17 | 8.86 |
| 2 | 3.90 | 28.01 | 8.31 |
| 3 | 6.10 | 31.66 | 11.00 |
| 4 | 8.35 | 47.91 | 13.68 |
| 5 | 10.15 | 55.97 | 14.46 |
| 6 | 12.35 | 57.59 | 16.78 |
| 7 | 14.65 | 73.08 | 33.88 |
| 8 | 17.15 | 52.70 | 21.74 |
| 9 | 19.15 | 52.00 | 13.54 |
| 10 | 22.25 | 7.79 | 4.30 |
| 11 | 24.55 | 7.13 | 3.81 |
| 12 | 28.15 | 8.70 | 5.66 |
| 13 | 29.85 | 9.08 | 5.76 |
| 14 | 32.05 | 11.04 | 5.93 |
| 15 | 34.45 | 22.12 | 13.20 |
| 16 | 36.65 | 13.30 | 12.25 |
| 17 | 39.85 | 18.11 | 10.40 |
| 18 | 44.25 | 19.33 | 13.19 |

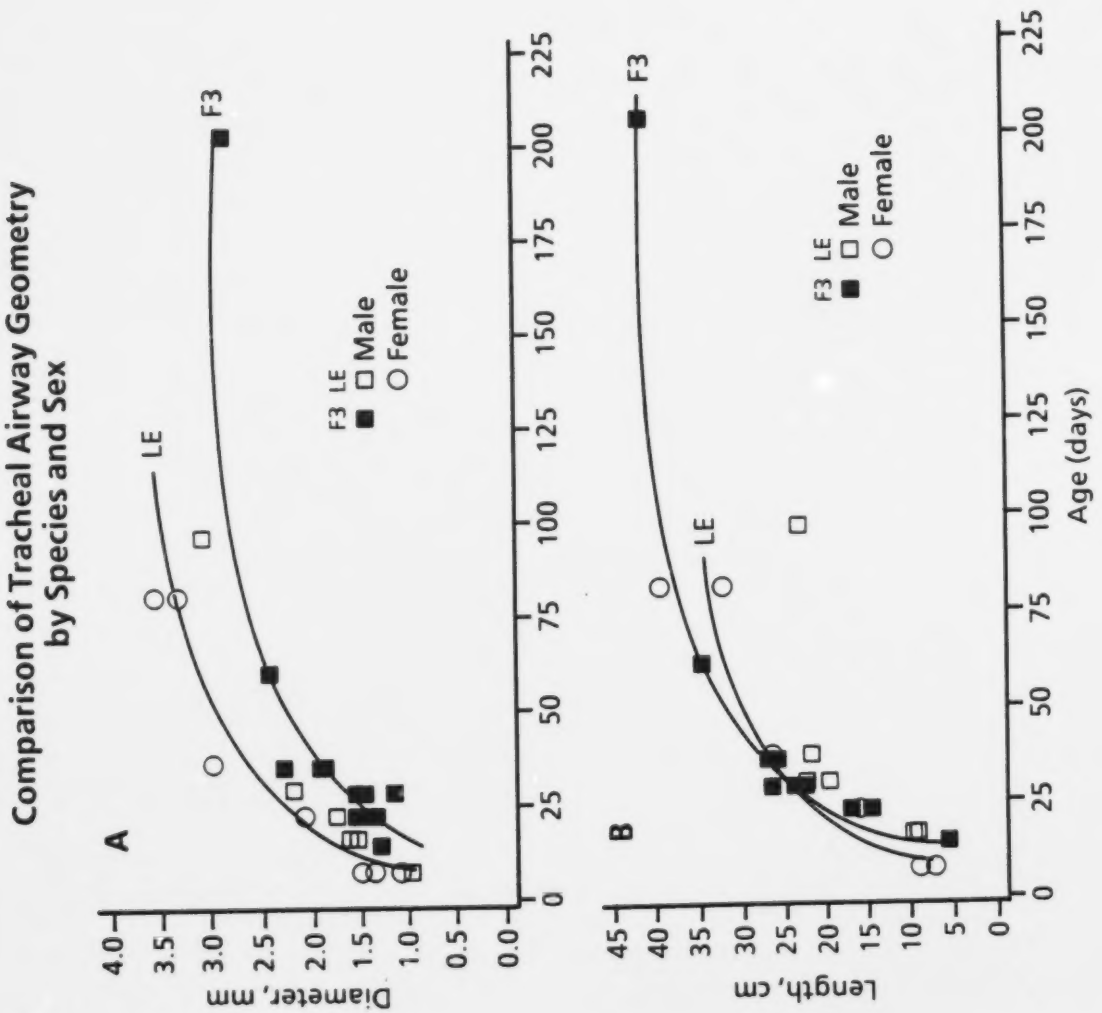


Figure 3. Tracheobronchial morphometry in the Fischer-344 rat and Long-Evans hooded rat as a function of growth. Panel A represents airway diameter, and Panel B represents airway length in the trachea.

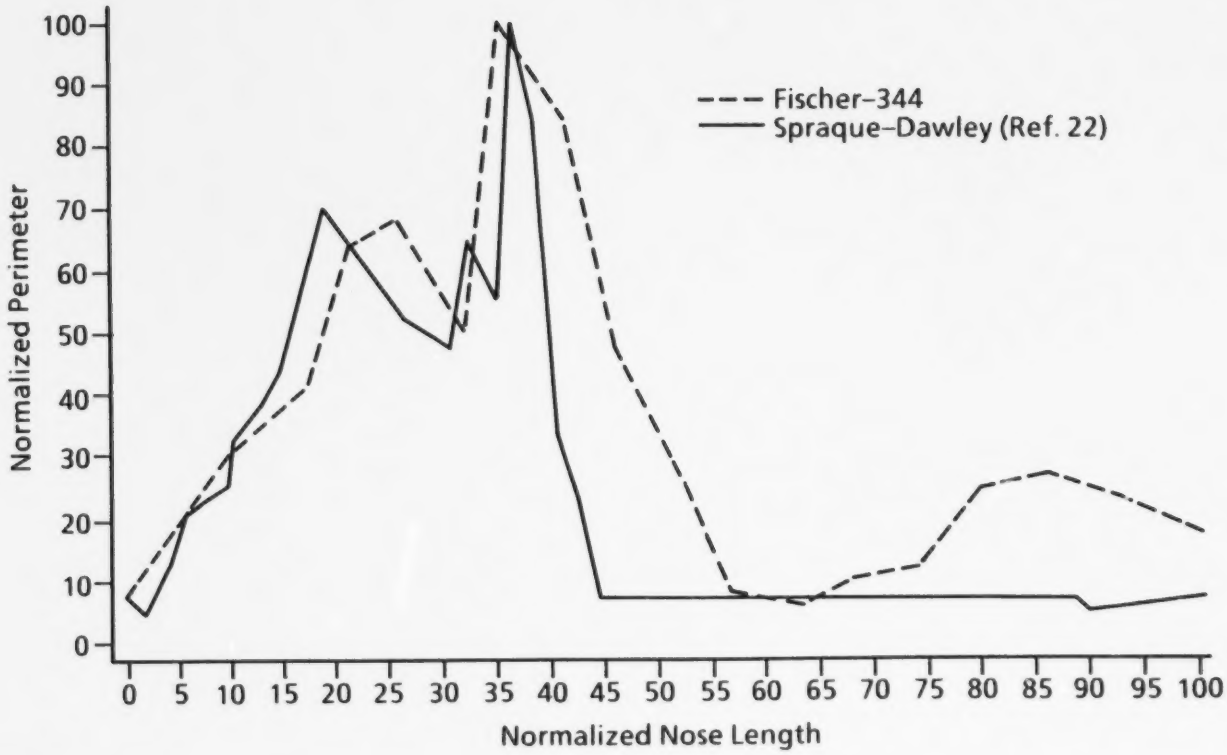


Figure 4. A plot of normalized perimeter vs. normalized nose distance for a Fischer-344 rat and Sprague-Dawley rat (from Ref. 22).

was measured and averaged over the same period of time. This process was repeated for inhalation and exhalation modes, in two mutually perpendicular directions.

A baboon nose cast was used to understand the potential effects of inhaled aerosols and efficiencies of collection in different nose locations. The hollow nose cast was exposed to a unidirectional flow of monodispersed particles, and captured particles were collected. Both inspiration and expiration models were considered. To examine the influence of tracheobronchial airway growth on particle deposition, morphometric data from the published work of Schlesinger et al. (20) and data measured in our laboratory were used as input into the deposition equations of Martonen (9). Table 3 lists these variables. Monodispersed particles of 7.6 μm and 3.0 μm in size were used for the deposition experiment. A density of 1.05 gm/cm$^3$ and a spherical shape with SD 2.0 μm and 0.02 μm were assumed. The particles were nebulized and captured inside the hollow models of the nose and lungs. The models were then cut up into the different airway branches and the deposited particles were counted by a high-speed electronic counter (Coulter Counter, Model 2F, Miami, FL). Collection efficiencies were calculated from the experimental findings and from theoretical models where available. Figure 5 shows the 7.6-μm particle size deposition efficiency for both inhalation and exhalation modes in a baboon nose cast. Figure 6 reveals the percentage particle deposition efficiencies for 7.6-μm and 7.7-μm particle sizes in a child and in an adult lung cast, respectively.

## RESULTS AND DISCUSSION

In a rat, the external nares are about 10% of the total length, while in a human and a baboon, these lengths are 12.1% and 22.4%, respectively. The maxilloturbinate region is 24.3% in a rat and 13.7% in a human; ethmoturbinate is 17.2% in a rat and 24.8% in a human; nasopharynx is 27.3% in a rat and 19.7% in a human; and larynx is 17.2% in length for a rat and 30.6% for a human. Evolution may have played a role in man's increased laryngeal region. In Figure 4, perimeters of the nose sections are plotted against the normalized length of the airway. The maximum perimeter at

**TABLE 3.** Morphometric measurements, particle and flow characteristics of the deposition experiments in hollow tracheobronchial casts

| Generation Number | No. of Branches Actually Used | Diam. (cm) | Length (cm) | Branching Angle (degrees) | Particles | Flow Q (lpm) |
|---|---|---|---|---|---|---|
| **Cast 1** | | | | | | |
| 0 | 1 | 1.437 | 13.3[a] | 0 | Diam. 7.6 µm SD = 2.0 µm | 25.0 |
| 1 | 2 | 0.981 | 3.25 | 33.5 | $\rho$ = 1.05 g/cm$^3$ | |
| 2 | 4 | 0.727 | 1.26 | 20.2 | | |
| 3 | 7 | 0.507 | 1.12 | 22.0 | | |
| 4 | 10 | 0.398 | 1.09 | 19.4 | | |
| **Cast 2 (Ref. 21)** | | | | | | |
| 0 | 1 | 1.75 | 10.6 | 0 | | |
| 1 | 2 | 1.39 | 3.15 | 24 | | |
| 2 | 4 | 0.95 | 1.65 | 33 | Diam. 7.7 µm SD = 0.02 µm | 30.0 |
| 3 | 8 | 0.69 | 1.28 | 28 | $\rho$ = 2.56 g/cm$^3$ | |
| 4 | 16 | 0.48 | 0.97 | 28 | | |
| 5 | 11 | 0.37 | 0.99 | 26 | | |
| 6 | 12 | 0.30 | 0.95 | 27 | | |

[a] Length includes larynx.

the ethmoturbinate region was considered to be 100 units of normalized perimeter. In all species for which data are available (22,12), the perimeter increases from the external nares to the maxilloturbinate region, and there is a sudden drop in the cross-sectional area and perimeter in the nasopharyngeal region. The effect of these area changes was considered responsible for residence time of airflow (13) in a baboon nose.

Visual examination of lung casts shows them to be of different patterns, including monopodial, dichotomous, and polychotomous. The number of lobes per lung also varied between species. Unlike the dichotomous lung airway branching, the monopodial lung branchings have short lateral branchings, attached with long tapering major bronchi at relatively large angles. The changes from non-alveolarized to alveolarized tissue are abrupt in some species (i.e., rat, mouse); while the transition is smooth in other species (i.e., man, monkey, etc). To describe the relationship between airway dimensions and growth, data were collected measuring length, diameter, and branching angles in groups of rats of different ages. Table 4 shows the population of animal characteristics used (24); length and diameter of the trachea are shown in Figure 3. An approximate sevenfold increase in length was seen in the first 100 days of growth. Growth in other conducting airways was not as spectacular. Airway diameters of the two species differed; not only was the diameter of the Fischer-344 rat trachea approximately 0.5 to 1.0 cm smaller than the Long-Evans rat trachea at all ages, but the increase with respect to age was also less dramatic. This pattern was seen throughout the airways of the right lung, but was less apparent in the left lung. It appears that an exponential model with an upper asymptote may be used to describe growth. Despite some differences in curvature and maybe some differences in the asymptotes between different species, this model appears to be valid for all airways.

A comparison of the cross sections of the nose cast of the rat reveals good agreement with published literature (24). The sudden drop in the cross-sectional area and perimeter may be responsible for slow airflow and high particle deposition efficiency in the nasopharyngeal region. Particle deposition was experimentally obtained by using a hollow replica cast of a baboon nose. A

**TABLE 4. Average velocities for a 1500-$cm^3/s$ flow rate calculated from thermistor probe measurements. Areas correspond to Figure 7[a]**

| Location | ID | Distance from the nares (mm) | Velocity[b] (cm/s) | |
|---|---|---|---|---|
| | | | Inhalation | Exhalation |
| External nares | A | 10.5 | 86.89 (8.68) | 47.76 (5.82) |
| | B | 30.0 | 86.63 (1.17) | 55.98 (0.48) |
| Maxilloturbinate region | C | 43.8 | 37.88 (16.82) | 40.62 (11.93) |
| | D | 59.3 | 34.95 (4.10) | 27.05 (14.54) |
| Ethmoturbinate region | E | 96.9 | 33.98(16.67) | 16.47 (3.45) |
| | F | 115.0 | 35.93 (4.56) | 14.11(7.15) |
| Nasopharynx | G | 132.5 | 20.95(10.07) | 8.77 (4.1) |
| Pharynx | H | 172.4 | 22.97(7.14) | 8.27(4.97) |
| Larynx | I | 205.3 | C | C |

[a]Data adopted from Ref. 13.

[b]Mean (standard deviation).

[c]Not available.

unidirectional flow of 25 lpm was used for the inhalation and exhalation modes separately. Once the particles were deposited, the model was split into multiple sections. The exact location of split sections are shown in Figure 7. Each section was placed in pre-measured isotonic water and sonicated for 30 min to dislodge the particles from the sections. After the particle concentrations were measured, the particle deposition efficiencies were calculated.

Figures 8 and 9 are the average velocity profiles for a 1500-$cm^3/s$ flow rate with the origin placed at the center of the passage. The inspiratory velocity profiles are shown in Figure 8, and the expiratory velocity profiles are shown in Figure 9. The velocity in Figure 8 starts with a parabolic profile and changes to M-shape, to turbulent, and again to parabolic at the exit. The velocity in the expiratory mode, on the other hand, starts as a bullet shape, to turbulent, to M-shape, to parabolic near the exit at the nares. The area under each curve was measured and the average velocity calculated. Table 4 lists these values. The relatively large magnitudes of some of the standard deviations with respect to their means can be attributed to the respective noncircular cross sections and mutually perpendicular velocity measurements.

The experimental particle deposition efficiencies in the nose are shown in Figure 5 for both inhalation and exhalation modes. For both modes the maximum percentage of deposition occurs in the ethmoturbinate region (Sections 5 and 6 in the figure). In the inhalation mode, once the flow passed this region, the amount of deposited particle decreased. The same pattern was seen in the exhalation model – as the flow passed the ethmoturbinate region (or olfactory region) and neared the tip of the nose, the amount of deposited particles decreased.

In the hollow lung casts, the experimental deposition efficiency of each generation was defined to be the ratio of particles deposited to the total particles entering the generation at the bifurcation regions. Figure 6 shows percent deposition efficiencies for two different particle sizes in two different lung models. Our experimental values of deposition in a child lung were compared to available published experimental data of NYU (20) on adult human lung casts. In all generations,

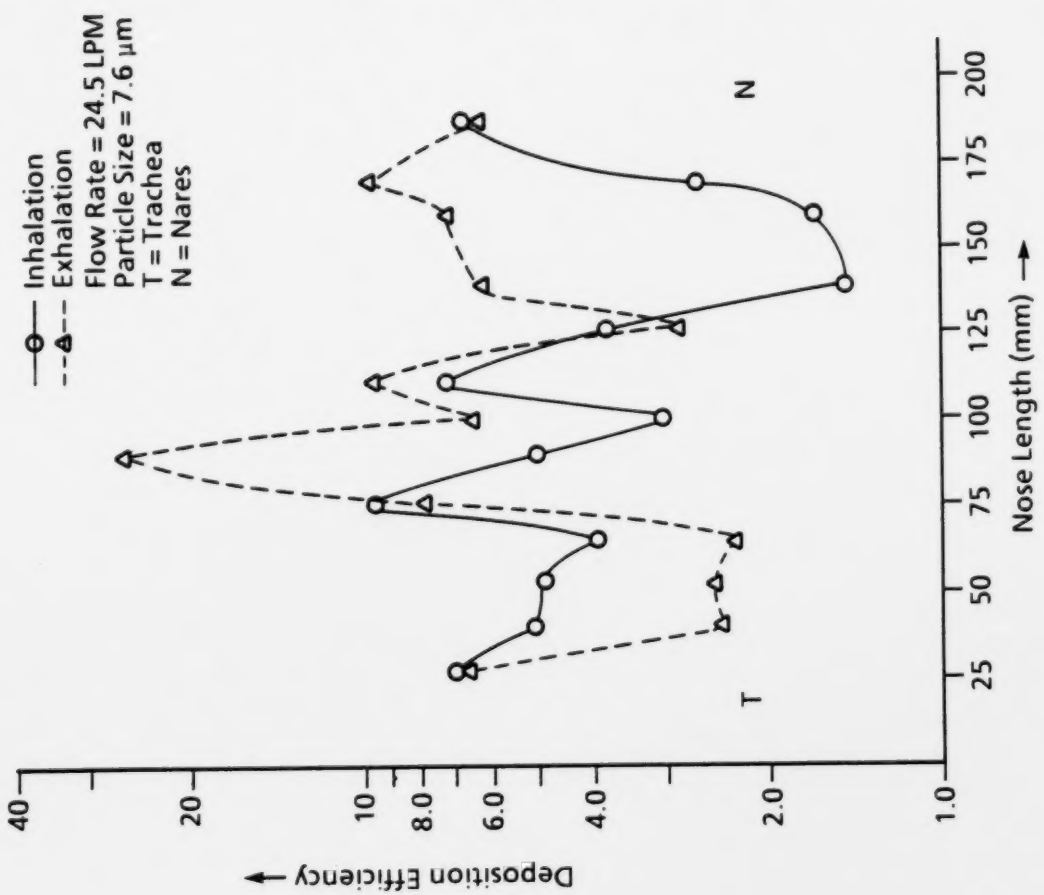


Figure 5. Particle deposition efficiencies as a function of location in a baboon nose cast.

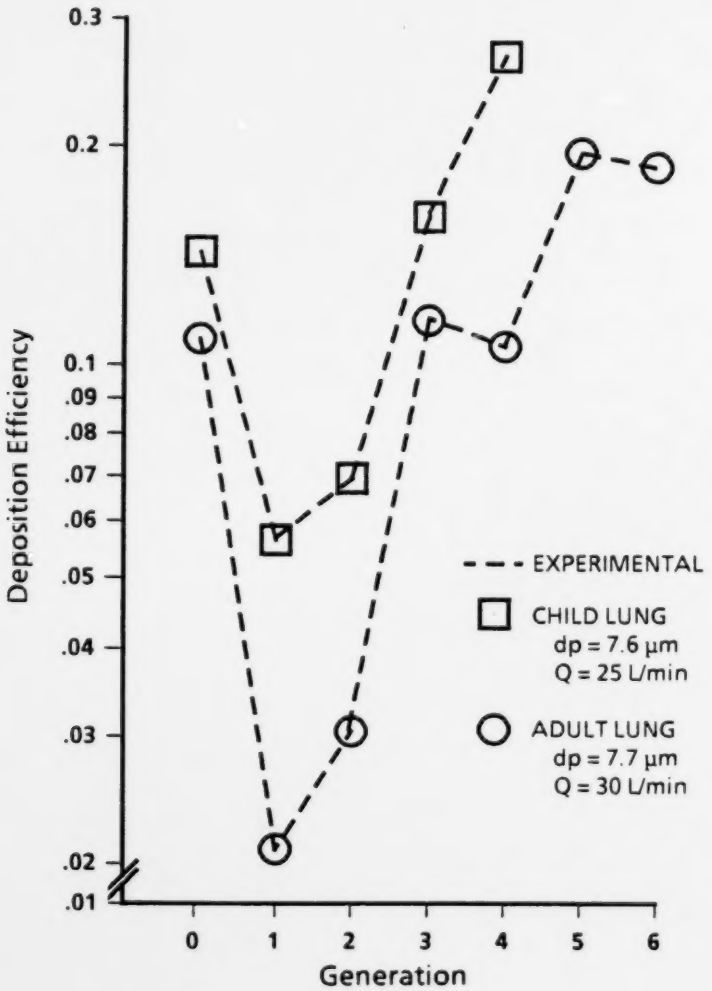


Fgure 6. Particle deposition efficiency in a child and an adult lung cast, as a function of generation number in a tracheobronchial tree.

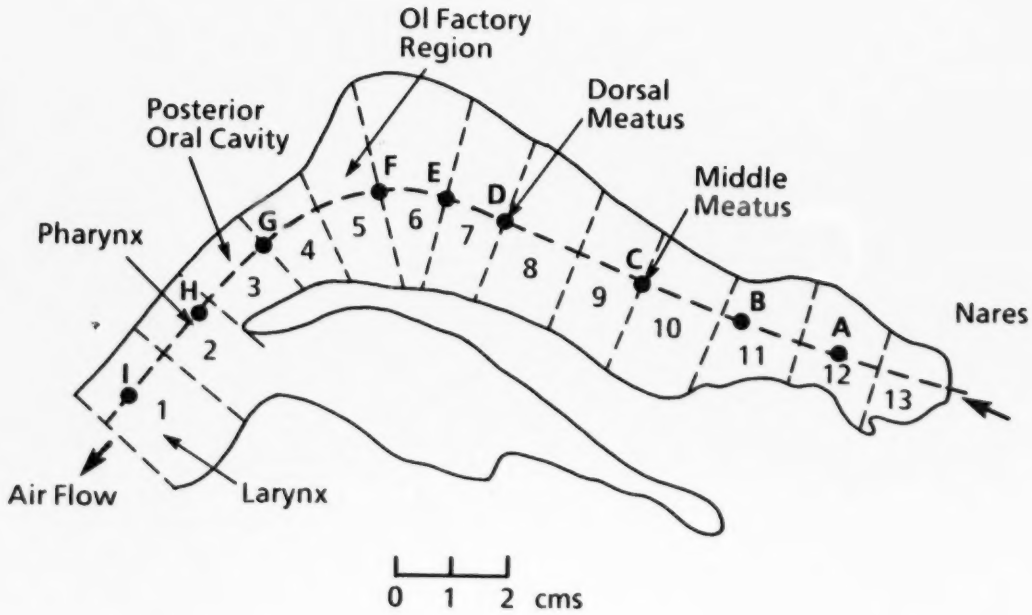


Figure 7. A line diagram showing the baboon nose cast sections where the deposition efficiencies are measured. Arrow shows the inhalation mode direction.

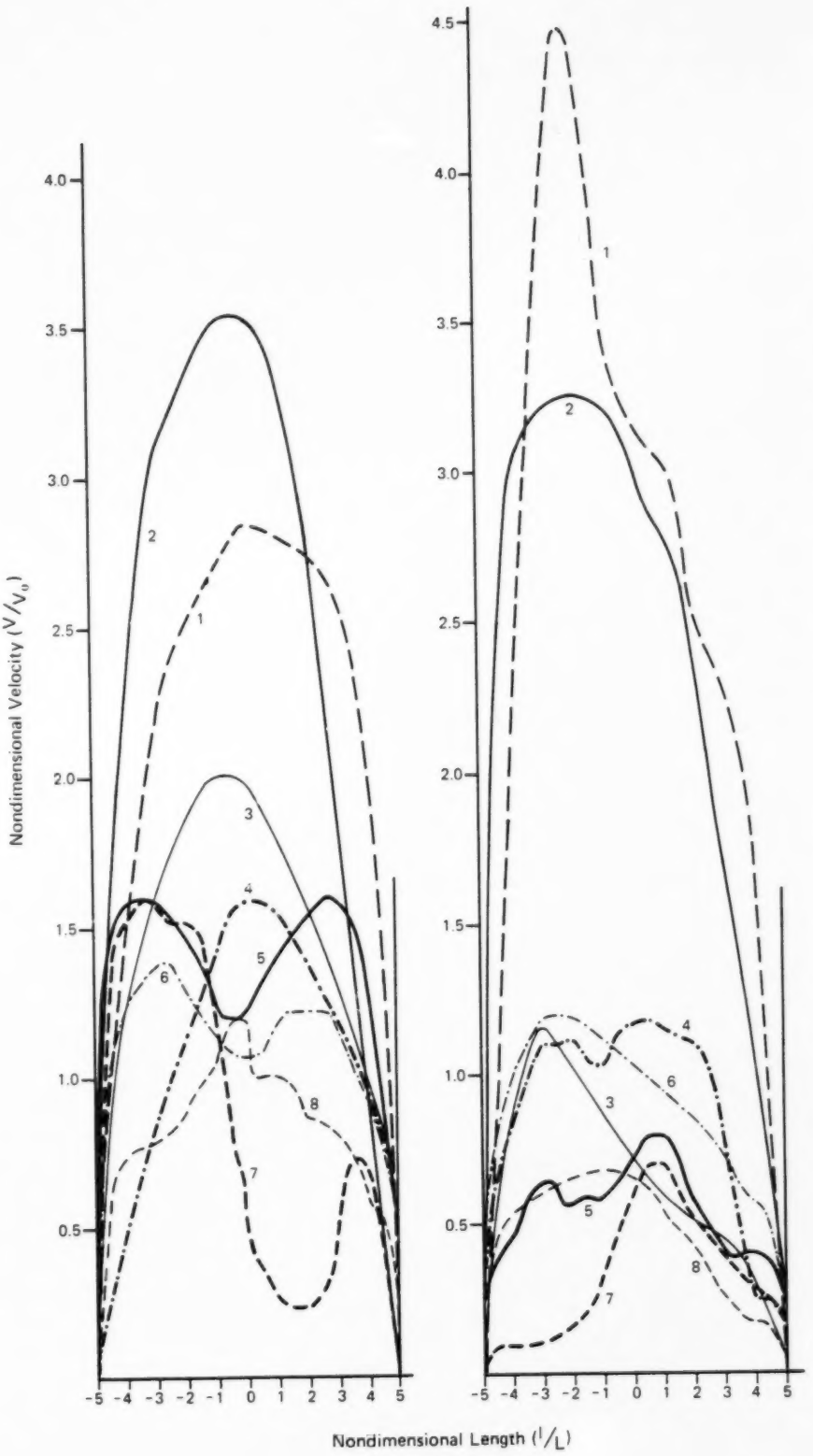


Figure 8. Nondimensional velocity distribution profiles in the nose for a 1500-$cm^3/s$ inspiratory flow rate plotted against nondimensional average length. Profile alphanumeric characters increase from tip of nose to larynx, and correspond to Figure 7. Panel A represents a plane perpendicular to the plane of paper traverse lines, and Panel B represents a plane along the plane of paper traverse lines.

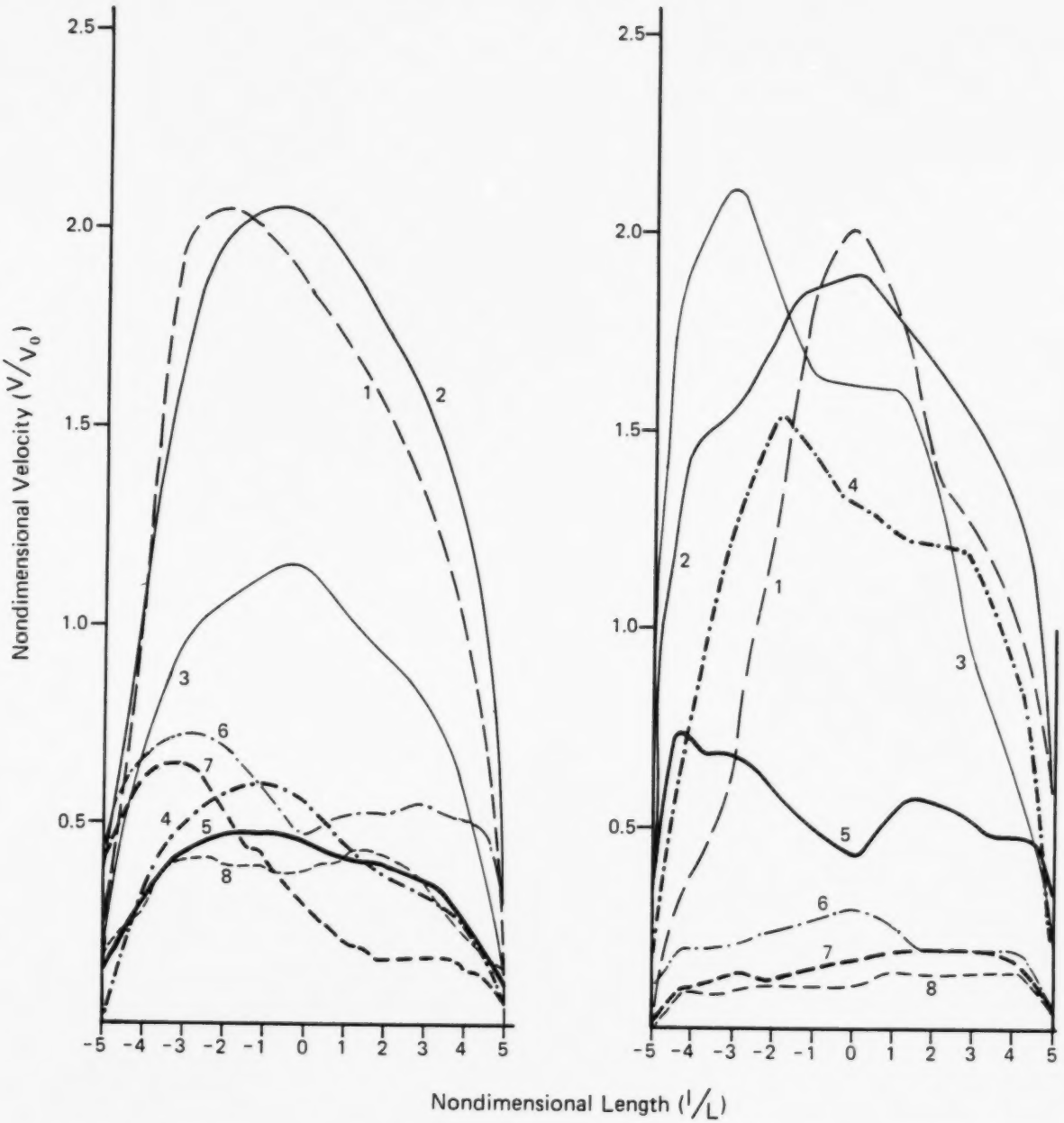


Figure 9. Nondimensional velocity distribution profiles in the nose for a 1500-cm³/s expiratory flow rate plotted against nondimensional average length. Profile alphanumeric characters increase from tip of nose to larynx, and correspond to Figure 7. Panel A represents a plane perpendicular to the plane of paper traverse lines, and Panel B represents a plane along the plane of paper traverse lines.

deposition efficiencies for child lung was found to be higher than in adult lung. Experimentally obtained deposition values were also observed to be higher than the theoretically calculated deposition efficiencies. This was true for all particle sizes (only 7.6 μm diameter of which is shown here) as expected, since airway morphometry is smaller in child than in adult lungs. The results of the present study suggest that child lung casts can be effectively used to understand the difference in deposition parameters in that subpopulation and to extrapolate data from adult to child lung deposition.

## CONCLUSIONS

This report describes methodology for developing replica casts of nasopharyngeal and tracheobronchial airways. Particle depositions in a hollow cast of the baboon nose and child (human) tracheobronchial tree are presented. The sections of nose casts measured in this study were compared with those measured by other investigators. The lung airways measured generally fell within reported range. Fractional particle deposition observed in both inhalation and exhalation modes in the nose appeared to be consistent among themselves. The efficiencies in the baboon and child lung casts and the similarities with published adult lung cast data show a possible basis for estimating the relative amount of inhaled particles that deposit at different generations of the tracheobronchial airways.

To investigate how particles affect deposition parameters, a replica cast can provide useful anatomical details not available through other means of experimentation. Flexible replica casts present methods for obtaining morphometric measurements necessary for mathematical modeling of particle deposition used to understand airflow and pressure drop characteristics in the airways.

Knowledge of airflow in a living specimen is difficult to achieve, and for this reason casts are used. A thermistor probe, because of its rigidness, is ideal for velocity measurements, but its slow response makes instantaneous velocity measurement impossible. For accurate predictions, use of a

wind tunnel with a steady flow is unavoidable. This study observed significant similarities to those observed by Girardin et al. (4).

The replica casts are realistic for experimental study of particle deposition, but the few limitations should be appreciated. The casts have realistic morphometry and can be designed to offer more detailed determination of piece by piece deposition data than is possible in an *in vivo* experiment. However, the realistic in and out airflow and mucus flow can hardly be achieved in a cast study, which neglects the effect of a clearance mechanism. In addition, the change of diameter and secondary effect of airflow due to heart beating may change the particle deposition pattern. The unidirectional airflow used in models to capture particles are at best conflicting. Bell (1) found that differences in deposition patterns result from an oscillating and unidirectional flow having the same mean value. As long as the limitations are recognized, the cast studies are excellent tools in which controlled exposure studies are not feasible. The inherent limitations with *in vivo* human research for susceptible subpopulations (child, persons with lung problems) make it difficult to determine pollutant dosimetric relationships for these groups. Replica cast models may be used to fill this void and provide a valuable complement.

**ACKNOWLEDGMENTS**

The author is indebted to Drs. D. Colvin (Triangle Research and Development Corporation, NC) and M. Knapp (Duke University, NC) for their help in obtaining the casts, to Mr. A. Gooya and Mr. N. Shaka for assistance in morphometric measurements, and to Ms. Ménache for statistical analysis.

**References**


1. Bell, K.A. (1978): Local particle deposition in respiratory airway models. In: *Recent Development in Aerosol Science*, edited by D.T. Shaw pp. 97-134. John Wiley and Sons, New York.

2. Clemente, C., editor (1985): *Anatomy of the Human Body*, 30th Edition. Lea and Febiger, Philadelphia.

3. Engel, S. (1962): Lung Structure. Charles C. Thomas, Springfield, Illinois.

4. Girardin, M., Bilgen, E., and Arbour, P. (1983): Experimental study of velocity fields in a human nasal fossa by laser anemometry. *Ann. Otol. Rhino. Laryngeal.*, 92:231-236.

5. Gooya, A., Shaka, N., Menache, M., and Patra, A. (1986): Growth of the major conducting airways in Fischer-344 and Long-Evans hooded rats. In: *Proceedings of 12 Northeast Bioengineering Conferences*. Yale, Connecticut.

6. Hofmann, W., Daschil, F., and Pohl, E. (1979): Animal lung models for the inhalation of natural radioactive particles and their relevance to man. In: *Proceedings of the 7th Conference Gesellschaft für Aerosol forschung*, edited by W. Stöber and R. Jaenicke, pp. 26-30. Dusseldorf, Germany.

7. Horsfield, K., and Cumming, G. (1967): Angles of branching and diameters of branches in the human bronchial tree. *Bull. Math. Biophys.*, 29:245-259.

8. Kliment, V. (1973): Similarity and dimensional analysis, evaluation of aerosol deposition in the lungs of laboratory animals and man. *Folia Morphol.*, 21:59-64.

9. Martonen, T.B. (1982): Analytical model of hygroscopic particle behavior in human airways. *Bull. Math. Biol.*, 44:425-442.

10. Montgomery, W., Vig, P., Stabb, E., and Matteson, S. (1979): Computed tomography: A three-dimensional study of the nasal airway. *Am. J. Orthod.*, 76:363-375.

11. Patra, A.L. (1986): Comparative anatomy of mammalian respiratory tracts: the naso-pharyngeal region and the tracheobronchial region. *J. Toxicol. Environ. Health*, 17:163-174.

12. Patra, A.L., Gooya, A., and Ménache, M.G. (1986): A morphometric comparison of nasopharyngeal airways of laboratory animals and human. *Anat. Rec.*, 215:42-50.

13. Patra, A.L., Gooya, A., and Morgan, K.T. (1986): Airflow characteristics in a baboon nasal passage cast, submitted to *J. Applied Physiol.*

14. Patra, A.L., Miller, F.J., and Graham, J.A. (1982): Development of breathing rat-lung models for particulate deposition studies. *Chem. Biomed. Environ. Instrum.*, 12(3):135-149.

15. Phalen, R.F., Oldham, M.J., Beaucage, C.B., Crocker, T.T., and Mortensen, J.D. (1985): Postnatal enlargement of human tracheobronchial airways and implications for particle deposition. *Anat. Rec.*, 212:368-380.

16. Phalen, R.F., Yeh, H.C., Raabe, O.G., and Velasquez, D.J. (1973): Casting the lungs *in situ*, *Anat. Rec.*, 177:255-263.

17. Raabe, O.G., Yeh, H.C., Schrum, G.M., and Phalen, R.F. (1976): Tracheobronchial geometry: human, dog, rat, hamster. LF-3, *Lovelace Foundation*, Albuquerque, NM.

18. Rahn, M., and Ross, B.B. (1957): Bronchial tree casts, lobe weights and anatomical dead space measurements in the dog's lung. *J. Appl. Physiol.*, 10:154-157.

19. Reznik, G., and Jensen, K. (1979): Anatomy of the nasal cavity of the European hamster. *Z. Versuchstierkuade*, 21:321-340.

20. Schlesinger, R.B., Bohning, D.E., Chan, T.L., and Lippman, M. (1977): Particle deposition in a hollow cast of the human tracheobronchial tree. *J. Aerosol Sci.*, 8:429-445.

21. Schlesinger, R.B., and Lippman, M. (1972): Particle deposition in casts of the human upper tracheobronchial tree. *Am. Ind. Hyg. Assoc. J.*, 33:237-261.

22. Schreider, J.P. (1986): Comparative anatomy and functions of the nasal passages. In: *Toxicology of the Nasal Passages*, edited by C.S. Barrow, pp. 1-25. MacGraw Hill, New York.

23. Schreider, J., and Hutchens, J. (1979): Particle deposition in the guinea pig respiratory tract. *J. Aerosol Sci.*, 10:599-607.

24. Schreider, J.O., and Raabe, O.G. (1981): Anatomy of the nasal-pharyngeal airways of experimental animals. *Anat. Rec.*, 200:195-205.

25. Timbrell, V., Bevan, N.E., Davies, A.S., and Munday, D.E. (1970): Hollow casts of lungs for experimental purposes. *Nature*, 255:97-98.

26. Weibel, E.R. (1963): In: *Morphometry of the Human Lung*. Academic Press Inc., New York.